Nat. Hazards Earth Syst. Sci., 23, 3407–3424, 2023
https://doi.org/10.5194/nhess-23-3407-2023

Natural Hazards and Earth System Sciences
Open Access
EGU

The footprint of a historical paleoearthquake: the sixth-century-CE event in the European western Southern Alps

Franz Livio[1], Maria Francesca Ferrario[1], Elisa Martinelli[1], Sahra Talamo[2], Silvia Cercatillo[2], and Alessandro Maria Michetti[1,3]

[1]Dipartimento di Scienza ed Alta Tecnologia, Università degli Studi dell'Insubria, Via Valleggio 11, 22100 Como (CO), Italy
[2]Department of Chemistry "Giacomo Ciamician", Alma Mater Studiorum, BRAVHO Radiocarbon Laboratory, University of Bologna, Via Selmi 2, 40126 Bologna (BO), Italy
[3]INGV, Osservatorio Vesuviano, Via Diocleziano 328, 80124 Naples, Italy

Correspondence: Franz Livio (franz.livio@uninsubria.it)

Received: 3 May 2023 – Discussion started: 3 July 2023
Accepted: 15 September 2023 – Published: 9 November 2023

Abstract. Low-deformation regions are characterized by long earthquake recurrence intervals. Here, it is fundamental to extend back the record of past events as much as possible to properly assess seismic hazards. Evidence from single sites or proxies may be not compelling, whereas we obtain a more substantial picture from the integration of paleo- and archeoseismic evidence at multiple sites, eventually supplemented with historical chronicles.

In the city of Como (N Italy), we perform stratigraphic and sedimentological analyses on the sedimentary sequences at Via Manzoni and we document earthquake archeological effects at the Roman baths by means of structure from motion and field surveys. Radiocarbon dating and chronological constraints from the archeological site allow us to bracket the time of occurrence of the deformations to the sixth century CE. We interpret the observed deformations as due to earthquake ground shaking and provide constraints on the lower threshold for the triggering of such evidence.

We move toward a regional view to infer possible relevant seismic sources by exploiting a dataset of published paleoseismic evidence in Swiss and N Italy lakes. We perform an inverse grid search to identify the magnitude and location of an earthquake that can explain all the positive and negative evidence consistent with the time interval of the event dated at Como.

Our results show that an earthquake (minimum M_w 6.32) with epicenter located at the border between Italy and Switzerland may account for all the observed effects; a similar event in the sixth century CE has not been documented so far by historical sources. Our study calls for the need to refine the characterization of the local seismic hazard, especially considering that this region seems unprepared to face the effects of an earthquake size similar to the one inferred for the sixth-century-CE event.

1 Introduction

Italy has one of the most complete and accurate historical seismic catalogues in the world, which can be considered complete for the last ca. 700 years for earthquakes of $M_w \geq 6.5$ in NW Italy (Rotondi and Garavaglia, 2002; Stucchi et al., 2004). Nonetheless, it is well known that oldest historical events (i.e., older than medieval times) can hardly be accurately recorded by historical sources and that the probability of incompleteness grows with age (Guidoboni et al., 2005). This is mostly true in settings where chronicles are clustered in a few cities and where human and natural events have possibly destroyed the records (Guidoboni et al., 2005) or where well-preserved archeological remains are sparse (e.g., high-mountain sectors in the core of the European Alps). In regions characterized by low deformation rates, an exceedingly long earthquake recurrence interval could possibly imply a lack of information regarding the strongest events, with a significant underestimation of the seismic hazard. Thus, the recognition of historical and prehistoric seismic events is essential for understanding the regional seismic potential of such regions.

Instead, natural and archeological records can be effective in filling the apparent gap in seismicity for oldest historical times. Some of the best examples are reported in studies on lake sediments, potentially able to image lake floor faulting or, more frequently, record large earthquakes as earthquake-triggered landslides and/or turbidites (e.g., Kremer et al., 2017, 2020; Oswald et al., 2021; Strasser et al., 2006, 2013). In the latter case, the paleoseismological significance of such evidence is inferred from the synchronicity of landslide events and from the spatial clustering in a certain region (Kremer et al., 2017). Nonetheless, the earthquake triggering and its age remain questionable or debated if age–depth models are flawed and considering that mass-wasting events obviously can also be triggered by climatic causes as well (Borgatti and Soldati, 2010; Trauth et al., 2003). Additional constraints on a possible seismic triggering would be furnished by onshore evidence that is less prone to concurrent triggering by other causes, and the consistency of both onshore and offshore data would provide an ideal integrated set of evidence for seismic triggering.

In this work, we present evidence from two sites in downtown Como, namely soft-sediment deformations in a stratigraphic sequence and disturbances in an archeological site. Then we look for coeval evidence, interpreted as paleoseismic, in lakes of the western Southern Alps. This allows us to provide a new hypothesis on the possible location of the seismic source and on the magnitude of the paleoearthquake.

2 Geological setting

2.1 Regional seismotectonics and historical seismicity

The city of Como is located at the margin of the European western Southern Alps, a sector of the Alps retro-wedge, bounded to the north and to the west by segments of the Periadriatic Lineament (Castellarin et al., 2006; Schmid and Kissling, 2000).

This area has been actively involved in the collisional phase of the Alpine orogeny since the Cenozoic (Castellarin et al., 2006; Handy et al., 2010; Scaramuzzo et al., 2022; Zanchetta et al., 2015) up to recent times (e.g., Sileo et al., 2007; Michetti et al., 2012). To the south, the active front of the Southern Alps fold-and-thrust belt lies presently buried beneath the Po Plain, facing the external arc of the Apennines with a relatively undeformed foreland in between the two chains (Fantoni et al., 2004; Scaramuzzo et al., 2022).

Across the western Southern Alps, shortening and seismicity rates significantly decrease westward (Fig. 1). Moderate seismic events hit the innermost sectors of the mountain chain during historical and early instrumental times. Figure 1b shows a cluster of similar events in the Valais region, mainly to the NW of the area (i.e., the 3 September 1295 Churwalden earthquake, M_w 6.2; the 9 December 1755 Brig-Naters earthquake, M_w 5.7; the 1855 Visp seismic sequence, max M_w 6.2; the January 1946 Sierre seismic sequence, max M_w 5.8; Rovida et al., 2016). Other moderate historical seismic clusters also occur to the east, along the piedmont belt of the Southern Alps. This includes the strongest events that hit the central and western Southern Alps and that can be regarded as the reference earthquakes for the whole region (the 25 December 1222 Brescia earthquake, M_w 5.68; the 26 November 1396 Monza earthquake, M_w 5.33; the 12 May, 1802 Valle dell'Oglio earthquake, M_w 5.6; Rovida et al., 2016). The seismic catalogues do not report any pre-medieval earthquake in the region.

Despite the relatively low rates of strain and seismic release, in the surroundings of the city of Como (Fig. 1), other sparse geological and geomorphological clues about recent seismic activity are reported, including both onshore (Sileo et al., 2007; Livio et al., 2011; Michetti et al., 2012) and offshore evidence (Fanetti et al., 2008; Kremer et al., 2020).

2.2 The Como urban area: geological and geomorphological setting, history and study sites

The Como urban area lies in a flat region at the end of the SW branch of Lake Como (Fig. 1); the plain is bordered by bedrock mountain slopes, comprising Mesozoic pelagic limestones (Medolo Group, Early Jurassic; Fig. 2) to the NE and deep-sea turbiditic conglomerates and sandstones (Gonfolite Group, Oligo-Miocene) to the SW (Michetti et al., 2014). The Gonfolite backthrust is a N-verging tectonic structure putting the Mesozoic succession in contact with the younger Gonfolite Group. Recent activity is documented by deformed Pliocene to Quaternary sediments (Bernoulli et al., 1989; Sileo et al., 2007). In the Como urban area, the fault was recognized during building excavations at the Borgovico site (Fig. 2); here, reverse surface faulting along a secondary splay of the backthrust involves Late Pleistocene to Holocene sediments (Livio et al., 2011).

The Cosia and Valduce creeks drain the plain, reaching Lake Como in the E and W sectors of the urban area, respectively; today, the final part of their course is buried beneath the city. The Como branch of the lake is hydrologically closed, since the only outlet is the Adda River, which outflows from the Lecco branch. During the Quaternary, the region was repeatedly occupied by glaciers. Given the local geomorphological setting and landscape evolution, the subsoil of the Como plain is composed of a sequence of fine, loose materials of lacustrine and fluvial origin, deposited since the late glacial period and throughout the Holocene. The environmental evolution of the study area has been reconstructed by means of stratigraphic, geotechnical and hydrogeological data; macro-remains and pollen analyses; and radiocarbon dating (e.g., Comerci et al., 2007; Ferrario et al., 2015; Martinelli et al., 2017).

The sedimentary sequence includes, at the base, inorganic clays settled in a proglacial lake following the last deglaciation. The lake level lowered progressively, allowing the de-

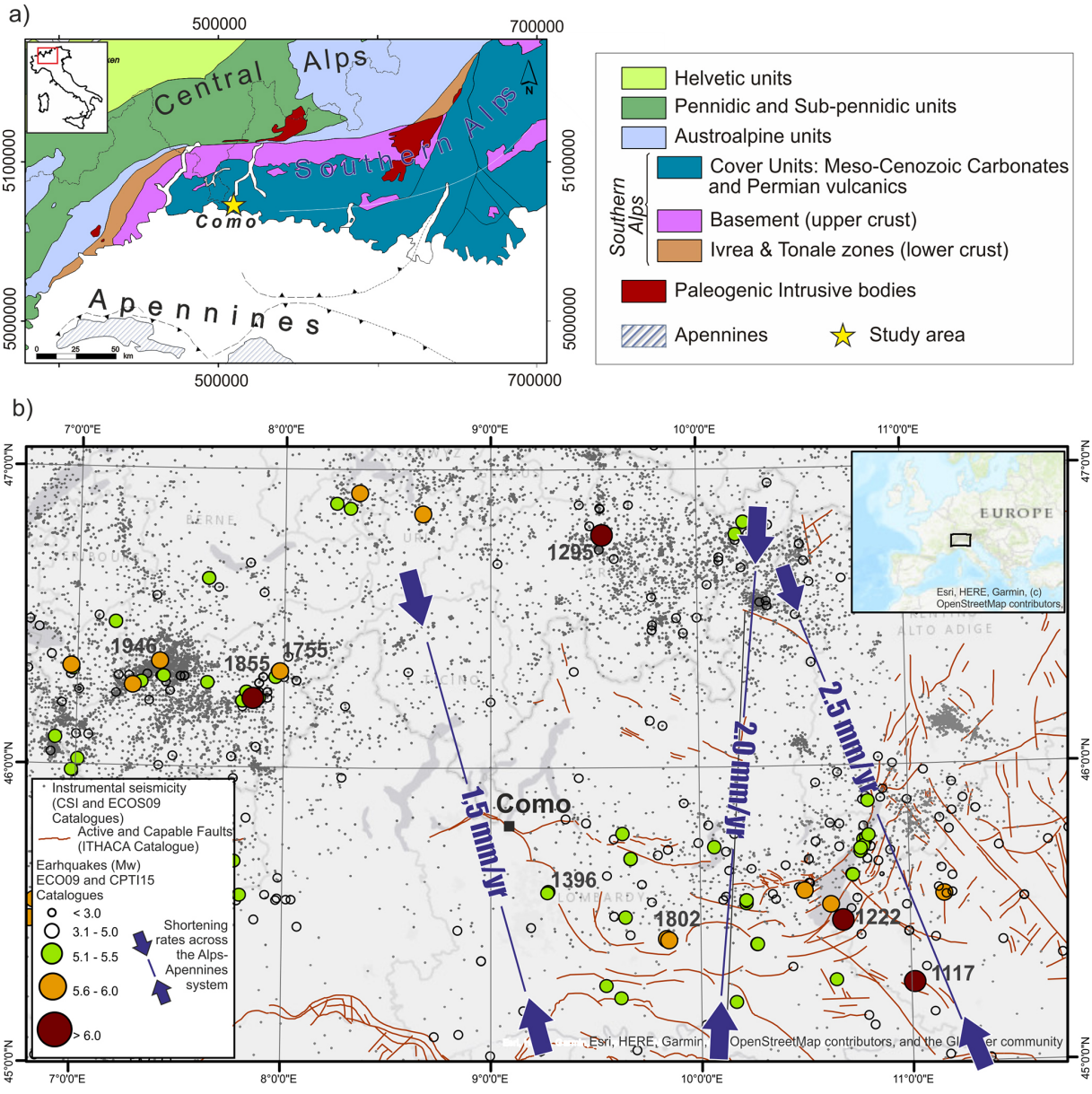

Figure 1. Geologic and seismotectonic setting for the study area: **(a)** geological sketch map of the Southern Alps; **(b)** circles show epicenters of instrumental and historical earthquakes (CPTI15 and ECOS09; Fäh et al., 2011; ISIDe Working Group, 2007; Rovida et al., 2016); red lines are active and capable faults according to the ITHACA database (Guerrieri et al., 2015; https://www.isprambiente.gov.it/en/projects/soil-and-territory/italy-hazards-from-capable-faulting-1?set_language=en, last access: 30 October 2023); shortening rates across the Alps–Apennines system are from Michetti et al. (2012).

velopment of a palustrine–lacustrine environment; this phase is attested by a thick sequence of sandy silts rich in organic remains (maximum thickness exceeds 40 m in the depocenter of the basin). During the Holocene, the basin was filled by alluvial deposits of the Cosia and Valduce creeks; the shallowest stratigraphic unit is constituted by 1–10 m of reworked materials, historical in age.

The presence of organic silts is the predisposing factor of the subsidence phenomena affecting Como town (Nappo et al., 2020). Subsidence rates are higher toward the lakeshore and at the center of the basin; due to groundwater overexploitation, subsidence reached critical rates (a few cm yr^{-1}) in the 1950s–1970s; water extraction has been forbidden since 1980, and today subsidence goes on at rates of a few millimeters per year, locally threatening the historical buildings (Nappo et al., 2021).

The oldest human occupation in the Lake Como area dates back to 60 000–50 000 cal yr BP, as suggested by sparse find-

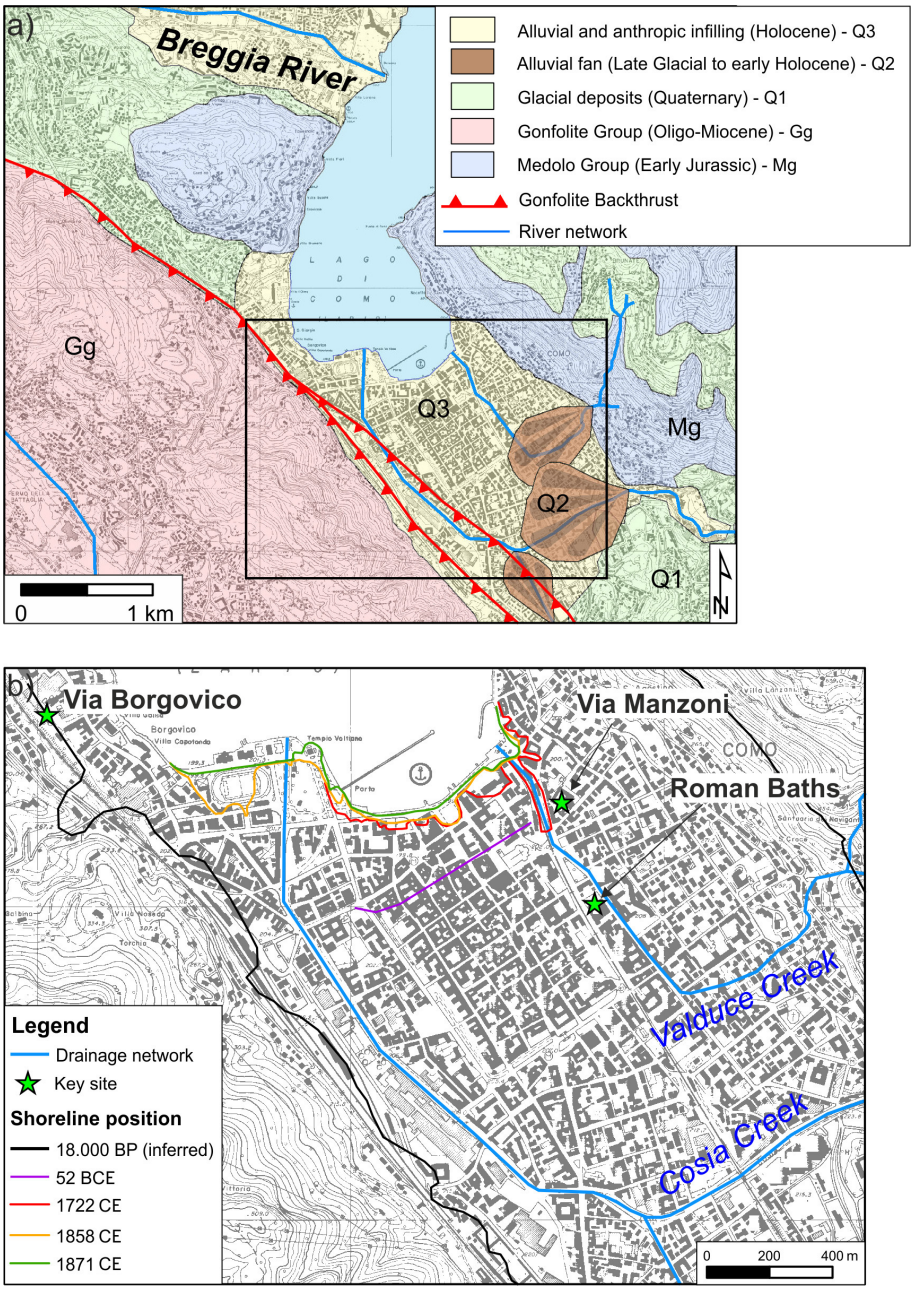

Figure 2. (a) Simplified geological and geomorphological setting of Como area (modified after Michetti et al., 2014); **(b)** river network and coastline position at different times (modified after Ferrario et al., 2015); basemap CTR (Carta Tecnica Regionale; 1 : 10 000 scale), after Regione Lombardia Viewer Geografico 2D – https://www.geoportale.regione.lombardia.it/ (last access: 30 October 2023).

ings of worked flints (Cremaschi, 2000); a more widespread occupation since the Mesolithic has been documented at several sites, in either the lowlands or the surrounding mountains (Casini, 1994; Castelletti and Motella De Carlo, 2012; Martinelli et al., 2017; Uboldi, 1993). During the Iron Age, the hills surrounding the Como plain were permanently inhabited (Martinelli et al., 2022; Uboldi, 1993), while the plain itself was occupied by a marsh and thus not suitable for human occupation. The plain is in a strategic position for trade along S–N routes, connecting the Po Plain and the rest of Italy with northern Europe; thus, the plain was reclaimed, and in the year 59 BCE Julius Caesar founded Novum Comum, the first settlement in the present-day Como urban area (Luraschi, 1997). Human interventions deeply modified the local environment, including the diversion of the Cosia creek. The coastline position progressively moved northward, firstly due to sediments supplied by the rivers and later due to anthropic land reclamation (Fig. 2). Since the Roman occupation of the

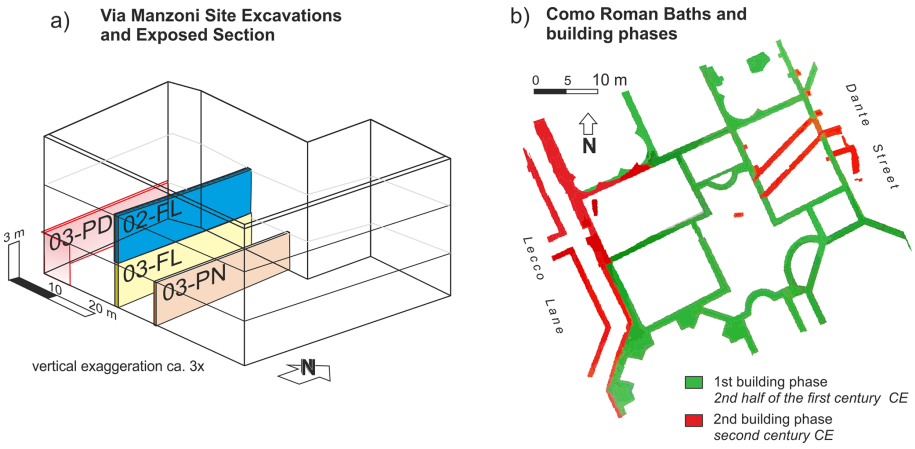

Figure 3. (a) Three-dimensional fence diagram with the location of the analyzed stratigraphic sections (codes are reported) – see the Supplement for a detailed description of each section; **(b)** map of the Como Roman baths with indications of the building phases (modified after Jorio, 2011).

plain, the local evolution has been the result of the interplay among natural processes and human control.

Archeological findings are widespread in the Como urban area (Uboldi, 1993), and here we focus on two sites, namely Via Manzoni and the Roman baths (Fig. 2b; Jorio, 2011), where archeo- and paleoseismic evidence has been discovered.

The Roman baths were unearthed in 1971, and then new excavations were completed in the early 2000s. The latest excavations at the Roman baths were conducted in 2009 under the scientific supervision of the Archeological Superintendence (Scientific Director: Stefania Jorio). The archeological site occupies more than 1500 m^2 and includes several edifices and a central courtyard, interpreted as the Roman baths of the town. Two building phases have been identified (Fig. 3b): the oldest dates back to the second half of the first century CE and the later one to the second century CE. An abandonment and dismantling phase that occurred in the fourth century CE is testified by a layer of alluvial deposits covering a ruin layer; the site was re-used in the fifth–sixth century CE as a burial place and finally covered by alluvial sediments.

At the Via Manzoni site, excavations were carried out in 2016 at a building site (Scientific Director: Lucia Mordeglia). Here, we could analyze the 3D setting of a 9 m thick sedimentary sequence, exposed in different sections.

3 Methods and materials

3.1 Stratigraphy and sedimentological analysis

We here provide a detailed description of some stratigraphic sections exposed by building excavations in the downtown Como area, at the Via Manzoni site. Figure 2 shows the location of excavations and the geometry and location of the outcropping sections. Excavations exposed a grid of vertical sections, from the depth of 3 m b.g.l. (below ground level) down to 9 m b.g.l. These sections provided a detailed stratigraphy covering the pre-Roman to historic time window in the shore environment of Lake Como. A detailed description of the sections is given in the Supplement.

We defined each stratigraphic unit based on macroscopic characteristics in terms of texture, fabric, grain size distribution and petrography, as well as content in macroscopic biological remains and/or archeological ones. If well recognizable in the field, we also considered unconformities and erosive surfaces.

3.2 Radiocarbon dating (^{14}C)

We selected 13 wood samples from the Via Manzoni site for radiocarbon dating. They were pretreated at the BRAVHO Radiocarbon Laboratory at Bologna University, and the cellulose was extracted following the procedure tested in Cercatillo et al. (2021). The BABAB (base–acid–base–acid–bleaching) protocol includes an initial overnight bath in 5 % NaOH, which cleans the sample of humic acids. The following steps include acidic (HCl 4%) and alkaline (NaOH 4 %) solutions and a final bleaching in 5 % $NaClO_2$. The entire procedure is carried out at 70 °C. When possible, at least 70 mg of wood was sampled (Table 1). Once the cellulose was dry (Table 1), an aliquot of 2.5–3 mg was put in aluminum cups and sent to the MAMS radiocarbon laboratory for graphitization and radiocarbon age determination. During the pretreatment two samples completely dissolved and for the other two the quantity of extracted cellulose was not sufficient for dating.

3.3 Mapping of archeoseismological evidence

We investigated the deformations and damage still preserved in the unearthed Roman baths of the city of Como (Fig. 2

Table 1. Dating results; the ^{14}C age and calibrated age (with an associated accuracy of 95 %) are reported, together with the sampling depth; the ^{14}C ages were calibrated using the IntCal20 calibration curve in the OxCal 4.4 program (Ramsey, 2009; Reimer et al., 2020). * Exact depth.

Unit	Lab. code	Start weight (mg)	Cellulose (mg)	^{14}C age (yr BP)	Calibrated age (year) (prob. 95 %)	Depth (m) (middle point of the layer)
02FL01	BRA5514	45.5	4.27	1467 ± 21	570–643 CE	−3.90
02FL05	BRA6056	67.9	5.4	1445 ± 24	582–651 CE	−4.64
02FL05	BRA5502	78.2	13.7	1426 ± 20	600–652 CE	−4.64
02FL08	BRA5515	87.1	4.9	1573 ± 19	430–551 CE	−5.20
02FL08	BRA5504	86	17.2	2116 ± 21	334–52 BCE	−5.20
03FL14	BRA5517	83.5	9.7	2550 ± 22	796–569 BCE	−6.12*
03FL18	BRA5518	75.9	3.6	2656 ± 23	894–793 BCE	−6.79*
03PN07	BRA5510	75.5	7.9	2488 ± 22	770–523 BCE	−6.60
03PN09	BRA5519	80.4	11	2529 ± 22	788–549 BCE	−7.26

for the location). For a description of the archeoseismological evidence, we follow the nomenclature and classification after Rodríguez-Pascua et al. (2011) and make a careful comparison with other similar effects described in the literature (e.g., Ferrater et al., 2015; Giner-Robles et al., 2009). We recorded the orientation and characteristics of each fracture measured in the baths' walls (i.e., dip azimuth and dip, sense of opening and aperture, presence of chipped corners, and orientation of the wall where the fracture lies).

A high-resolution point cloud model of the Roman baths has been obtained thanks to a structure from motion–multi-view stereo workflow (e.g., Gallup et al., 2007; Goesele et al., 2007; Westoby et al., 2012).

We shot 1043 digital photos in RAW format with a Nikon D5200 reflex camera equipped with a 35 mm optical lens, allowing us to minimize the lens distortions. We checked the internal accuracy of the model by means of 21 ground control points that were geotagged in the field and in the 3D model.

We processed all the photos with Agisoft Metashape software, resulting in a highly accurate 3D point cloud, with an average spacing of 0.5 cm along the baths' walls.

The obtained dense point cloud was finally processed in CloudCompare software and in QGIS in order to extract points included in narrow fences (profiles), remove outliers and interpolate in a mesh with a Delaunay triangulated irregular network (TIN) interpolation. Finally, values of the dip and dip direction of each face of the interpolated mesh have been analyzed in a stereonet plot to detect subtle folding of originally horizontal reference surfaces.

3.4 GIS buffer analysis for source location: issues for the assignment of macroseismic intensity and magnitude

To provide a regional view, we compared the age of the studied earthquake-induced effects with other coeval evidence known in the Alpine area. To date, the best available database covering the Holocene and historic time window is the Database of the Potential Paleoseismic Evidence in Switzerland (Kremer et al., 2020).

We listed all the evidence within a reasonable distance (i.e., 150 km) and considered synchronous those pieces of evidence whose age (i.e., whenever the age of the event was within a 2σ confidence bound) overlapped with the upper and lower age limits of the event recorded in Como. We here recall that the ages calculated in Kremer et al. (2020) are based on age–depth models with a linear interpolation between the closest dated samples and using an "event-corrected depth", i.e., on sediment depth subtracted from the thickness of sediment layers attributed to events (considered "instantaneous" layers relatively to the "normal" background sedimentation). In the GIS analysis that will follow, these locations are defined as "positive-evidence" data points. On the other hand, those locations where a well-documented stratigraphic sequence is available but coeval evidence of an earthquake-induced effect is lacking are defined as "negative-evidence" data points. As a preliminary step for a GIS analysis, all the positive and negative evidence for a synchronous effect, triggered by the same earthquake, is collected.

The adopted GIS buffer analysis is largely based on the grid-search approach after the early work by Bakun and Wentworth (1997) and fully described in Kremer et al. (2017). The workflow relies on the adoption of an empirical intensity–attenuation relationship for evaluating how intensity is decreasing with distance and on the assumption of a threshold intensity for the triggering of the considered effect.

The GIS buffer analysis consists of two steps: first all the locations with positive evidence are inverted to calculate the magnitude of the event that could have triggered the effect at increasing distances; then all locations with negative evidence are used to back-calculate the estimated local intensity

at those sites, given the results of the first step. Each grid cell where the back-calculated intensity exceeds the threshold is thus excluded. Actually, we postulated a lower- and an upper-threshold intensity value for triggering the considered effect. Lower-threshold values need to be exceeded at positive-evidence locations; on the contrary, upper-threshold values have to not be exceeded at negative sites (see a detailed discussion in Kremer et al., 2017).

Following the sensitivity analysis performed by Kremer et al. (2017), we solved the equations by assuming a lower-threshold intensity value for mass-wasting-movement triggering of intensity $VI_{2/10}$. Upper-threshold intensity has been fixed at $VI_{5/10}$, allowing a certain degree of uncertainty due to the possible epistemic errors in associating positive or negative evidence for such old events. We here underline that changes in the lower-threshold intensities for the positive evidence will result in different estimates of the inverted magnitude but with similar spatial distributions. Conversely, increasing or reducing the upper-threshold value will result in a reduction or increase, respectively, of the area potentially hosting the seismogenic source.

Following other similar studies (Strasser et al., 2006, 2013; Kremer et al., 2017; Oswald et al., 2021), we adopted the attenuation regression specifically developed by Fäh et al. (2011) for deep Alpine earthquakes.

For epicentral distances < 55 km,

$$I = -2.8941 + 1.7196 M_{\mathrm{w}} - 0.03 D, \quad (1)$$

and for epicentral distances > 55 km,

$$I = -4.2041 + 1.7196 M_{\mathrm{w}} - 0.0064 D, \quad (2)$$

where I is the local intensity (EMS-98 intensity scale), M_{w} is the earthquake moment magnitude and D is the epicentral distance (km).

During the first step of the analysis, a grid-search approach inverts the lower threshold at the location of the positive evidence to the corresponding M_{w} that should be obtained over a grid of trial source locations (Bakun and Wentworth, 1997), using the empirical intensity–attenuation relationships in Eqs. (1) and (2). This procedure is applied to all the positive-evidence data points.

Then all the obtained grids of possible M_{w} values are stacked and the maximum M_{w} value among all the grids is sampled. The grid obtained from this process represents the minimum M_{w} value of a hypothetical earthquake that is consistent with the triggering of the effects observed at all the positive-evidence data points (positive-evidence grid).

During the second step of the analysis, the same procedure is applied for the negative-evidence data points, using the upper-threshold intensity value instead. The obtained grid represents a maximum value of M_{w}, for each location, not to be exceeded in order not to trigger effects at the negative-evidence sites (negative-evidence grid). The positive-evidence grid is finally compared with the negative-evidence grid: all the cells where the former exceeds the latter are excluded from the final result of the analysis.

4 Evidence observed at the city of Como

4.1 Via Manzoni site

The Via Manzoni site exposed a sequence of mainly fine-grained and fining-upward units down to the depth of 9 m b.g.l. Figure 3a shows the relative position of the four investigated sections, while Fig. 4 illustrates the composite stratigraphic column. The stratigraphy from the ground level down to 3 m b.g.l. has not been documented, but archeological observations constrain the age of that interval to between the modern age and medieval times (Paul Blockley, personal communication, 2022).

Section 02FL records the stratigraphy between the depth of 3 and 6 m b.g.l. It is composed of two fining-upward cycles from clast-supported gravels in a sandy matrix to finely laminated fine sands alternating with silty loams rich in biological remains. The depositional environment is an alluvial plain with overbank deposits alternating with fluvial channels and passing upward to a palustrine and lacustrine setting. Each cycle is relative to a progressive ingression of the shore and lacustrine environment onto the alluvial and fluvial one due to a fast-subsiding setting, followed by episodes of alluvial aggradation by flooding events.

The base of the upper cycle is marked by laminated silty fine sands affected by fluidification and soft-sediment deformation features (convolution features, above, and balls and pillow structures, below; Fig. 4c) for a thickness of ca. 1 m. These beds appear to be entirely fluidized, and thus they are interpreted as a single event of fluidization. The top of the fluidized interval lies below a pack of coarse gravels with load structures deforming the base of the gravels and both the underlying bed and the convoluted laminae as well (Fig. 4d). Following Owen et al. (2011), a context-based approach has allowed us to exclude other triggering factors (e.g., storm waves, tsunamis, tidal shear, periglacial processes and groundwater seepage) and to also exclude possible deformations due to a sudden vertical load caused by the deposition of a coarse bed onto saturated sands. The only load deformation structures, clearly visible in the sequence at the top of the fluidized bed, are in fact deforming the convoluted bed and thus postdating the fluidization.

The sequence continues downward with several cycles of fine beds alternating with coarse ones and with an overall coarsening downward trend. Section 03 FL is partially overlapping and correlated with Section 03 PN, outcropping nearby and exposing 3 m of slightly inclined beds (N34/16), which we ascribe to the same depositional environment.

Section 03 PD is outcropping a few meters to the west of the FL one (Fig. 3a). It exposes a sequence of foreset beds,

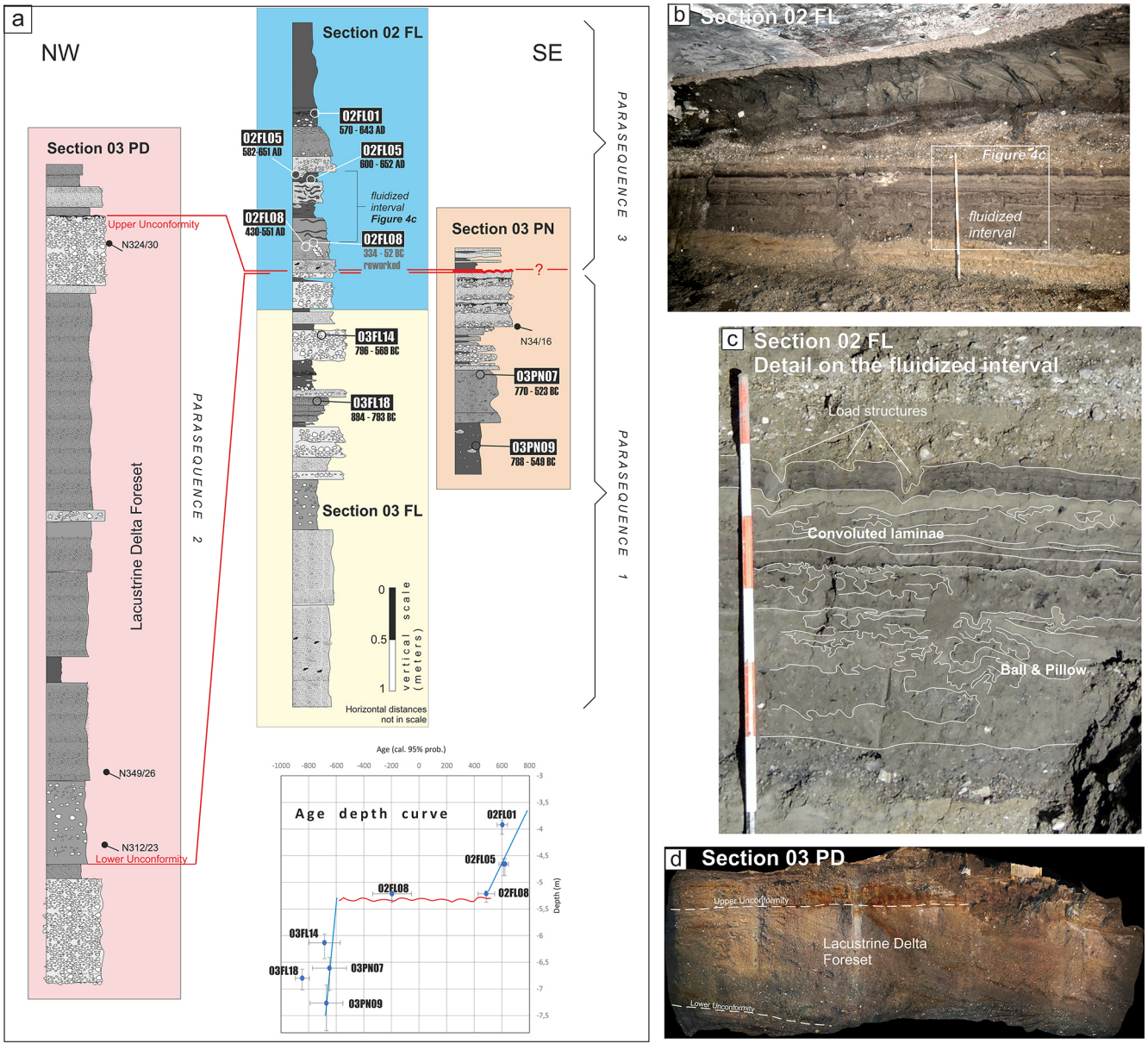

Figure 4. **(a)** Composite stratigraphic section for the Via Manzoni site: samples for ^{14}C dating and age results are reported (unit code in the black rectangles and calibrated ages with 95 % probability – see the Supplement for a detailed log; **(b)** perspective on the 02FL section; **(c)** interpreted detail of the fluidized interval within the sequence; **(d)** perspective on the 03PD section, showing the two angular unconformities bounding a pack of lacustrine delta foreset beds.

moderately inclined toward the lake, bounded at the base and at the top by two unconformity surfaces and representing a progradation event of a lacustrine delta (Fig. 4d). The top of the delta is correlative with the base of Section 02FL, as confirmed and precisely defined by the dating.

The nine dated samples within the sequence (Table 1) allow us to ascribe the entire documented stratigraphy to a period between the ninth century BCE and the seventh century CE. The age–depth model (Fig. 4) indicates that there is a major unconformity that can approximately be located at the depth of 5.20 m b.g.l., that is, close to the base of the fluidized level. In this line, we were able to define three parasequences that compose the Via Manzoni stratigraphy. The base of the uppermost parasequence (Parasequence 3 in Fig. 4) is marked by a maximum flooding surface that represents the transition from aggradation (Parasequence 1) to regression in the system due to the ongoing subsidence of the Como basin. The hiatus at the maximum flooding surface laterally corresponds to the growth of the lacustrine delta (Parasequence 2), which can be consistently ascribable to a

period between ca. the seventh century BCE and the fifth to sixth centuries CE, even if lacking direct dating.

From the evidence above, we can finally assess that (i) the fluidization observed in Section 02FL is triggered by ground shaking and (ii) the event is chronologically constrained at the boundary between the sixth and seventh century CE, most probably at the end of the sixth century CE. The lower age bound comes from the minimum age of the 02FL08 sample dating, i.e., the lowermost deformed unit, whereas the upper age bound is given by the maximum age of the 02FL05 sample. If we consider these constraints, we obtain a possible event age of 430–652 cal yr CE. Nonetheless, a more constrained age is estimated by considering the inner bounds from the age coming from dating: 551–582 cal yr CE. This age constrain comes from the assumption that the completely fluidized interval has been deformed by a single event. This assumption is reasonable considering that all the beds in the fluidized interval are deformed.

4.2 Roman baths' site

The Roman baths preserve some peculiar damage on the walls and structures that can be interpreted as earthquake archeological effects (EAEs, sensu Rodríguez-Pascua et al., 2011; Fig. 5).

A preserved arch shows evidence of partial collapse (Fig. 5b) and stone movements, possibly caused by the repeated shaking of non-collapsed walls. An entire wall section, which was presumably originally placed at ca. 2 m of height, is presently sticking out of the ground, in vertical position, right next to its original location (Fig. 5c). The wall collapsed onto a layer of alluvial sediments that were deposited at the site after its definitive abandonment, most probably when the fifth–sixth-century-CE tombs were excavated at the site.

Building stones are affected by several corner chips and fractures which either crosscut single stones or pervasively run across entire walls. We measured 205 fractures in the site, including features cutting through the stones and the mortar, recording the orientation of fracture at chipped corners and the aperture of the fractures as well. Widening downward fractures are particularly indicative of archeoseismology, since these are hardly caused by differential compaction of soil. Fracture orientation (Fig. 6) indicates that the most frequent strike orientations are N30 and N110, with a secondary prevalence of N90 and N170 striking fractures. These directions are oblique to those ones of the baths' walls (i.e., N80 and N170), allowing us to exclude the possibility that the observed damage is mainly due to the walls' settlement through time.

A section of the walls showed evidence for very subtle folding and of restoring interventions through time. The stone rows at this site are irregular; an additional row of stones has been added at the beginning of the second building phase. Analysis of the high-resolution 3D models of the baths allowed us to extract a mesh model for each stone row and to analyze subtle folding and deformations (Fig. 6e and f). We observe that the wall is gently folded along an antiform with a subvertical axial plane striking ca. NE–SW, consistently with the strike of the main fracture sets we measured.

Some of the observed damage at the Roman baths could also be due to the effects of (i) a differential compaction caused by subsidence (i.e., fractures in the walls and gentle folding) and (ii) damage due to the shallow depth of the ruins, below a former gas station (partially collapsed arch). Chipped stone corners are more probably linked to ground shaking, and, most importantly, the collapsed wall, stuck in a vertical position right next to its original location, is not consistent with any toppling-like kinematics due to typical wall collapse.

4.3 The footprint of the sixth-century-CE event

The investigations at downtown Como allow for identifying the occurrence of at least one paleoseismic event that triggered the effects observed and described at the city of Como: hereafter we will refer to this historical earthquake as the sixth-century-CE event. The lack of any historical account for such an event prevents any investigation in this sense. Nonetheless, it is reasonable that the shaking of the same earthquake could have produced similar effects in other sites where the geological and geomorphological setting is particularly sensitive to earthquake-induced secondary effects. Previously, studies on the lacustrine stratigraphic records in the Alps as natural "seismometers" (e.g., Oswald et al., 2021; Strasser et al., 2006, 2013) offered consistent results for historical earthquakes and opened the possibility of quantitatively exploring the occurrence of prehistorical events.

We evaluate this hypothesis by incorporating in our analysis surrounding sites that present positive and negative evidence; we considered the Swiss database (Kremer et al., 2020), supplemented with more recent publications (e.g., Nigg et al., 2021; Rapuc et al., 2022). Figure 7 shows the location of the sites, while Table 2 presents a summary of the available information for positive evidence.

Lake sediments act as natural seismographs, since they may archive information on seismic shaking that occurred in the past (Strasser et al., 2013). The stratigraphy of lake sediments can be investigated using high-resolution geophysical surveys, often supplemented by core drillings, to obtain ground-truth seismic data and to recover datable material. Mass-transport deposits (MTDs) are easily recognized in seismic data due to their chaotic facies, in stark contrast to the regularly laminated undisturbed sediments.

Extensive investigations have been performed on the northern side of the Alps (e.g., Monecke et al., 2006; Strasser et al., 2006, 2013; Beck, 2009). A dataset of paleoseismic evidence in Switzerland and conterminous regions has recently been presented by Kremer et al. (2020). Paleoseismic evidence is not randomly distributed through time but is clus-

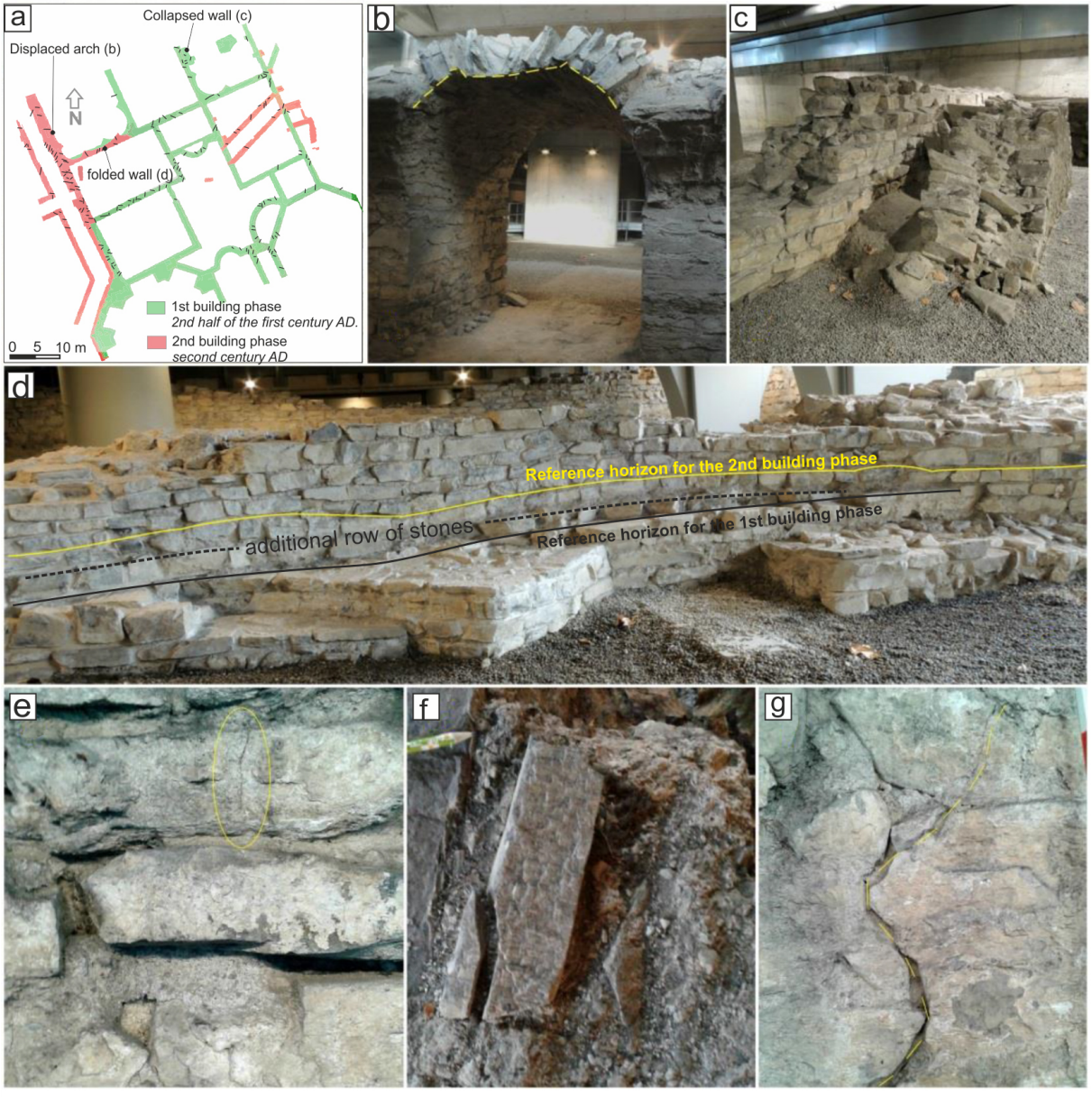

Figure 5. Potential earthquake-induced archeoseismological effects surveyed at the Como Roman baths: **(a)** map with the location of the observed features highlighted; **(b)** collapsed arch with displaced stones; **(c)** collapsed wall, view from the east; **(d)** a well-preserved section of the walls showing very subtle evidence of folding – a line of stones showing the loss of horizontality has been highlighted; **(e)** fractures in single stone blocks; **(f)** chipped corners; and **(g)** penetrative fractures cutting through the stones and the mortar.

tered at specific dates; in particular, enhanced seismic activity is documented at ca. 9700 and 6500 cal yr BP and in the last 4000 cal yr BP (Strasser et al., 2013; Kremer et al., 2020).

The southern side of the Alps has been investigated less systematically; nevertheless, some studies have identified turbidites in lake deposits. Such MTDs have been tentatively associated with seismic shaking.

Fanetti et al. (2008) performed limno-geological investigations in Lake Como, including a bathymetric survey, high-resolution seismic reflection studies and gravity core analyses. They identified two megaturbidite bodies, up to 3.5 m thick, interpreted as the result of large debris flows originating from the northern part of the Lake Como branch. The oldest deposit has a volume of ca. 10×10^6 m^3, while the upper deposit has a volume of 3×10^6 m^3. Chronological constraints are not well substantiated, but extrapolation of mean sedimentation rates obtained from ^{137}Cs and ^{14}C dating allows us to infer a tentative age of the sixth and twelfth century CE for the two deposits.

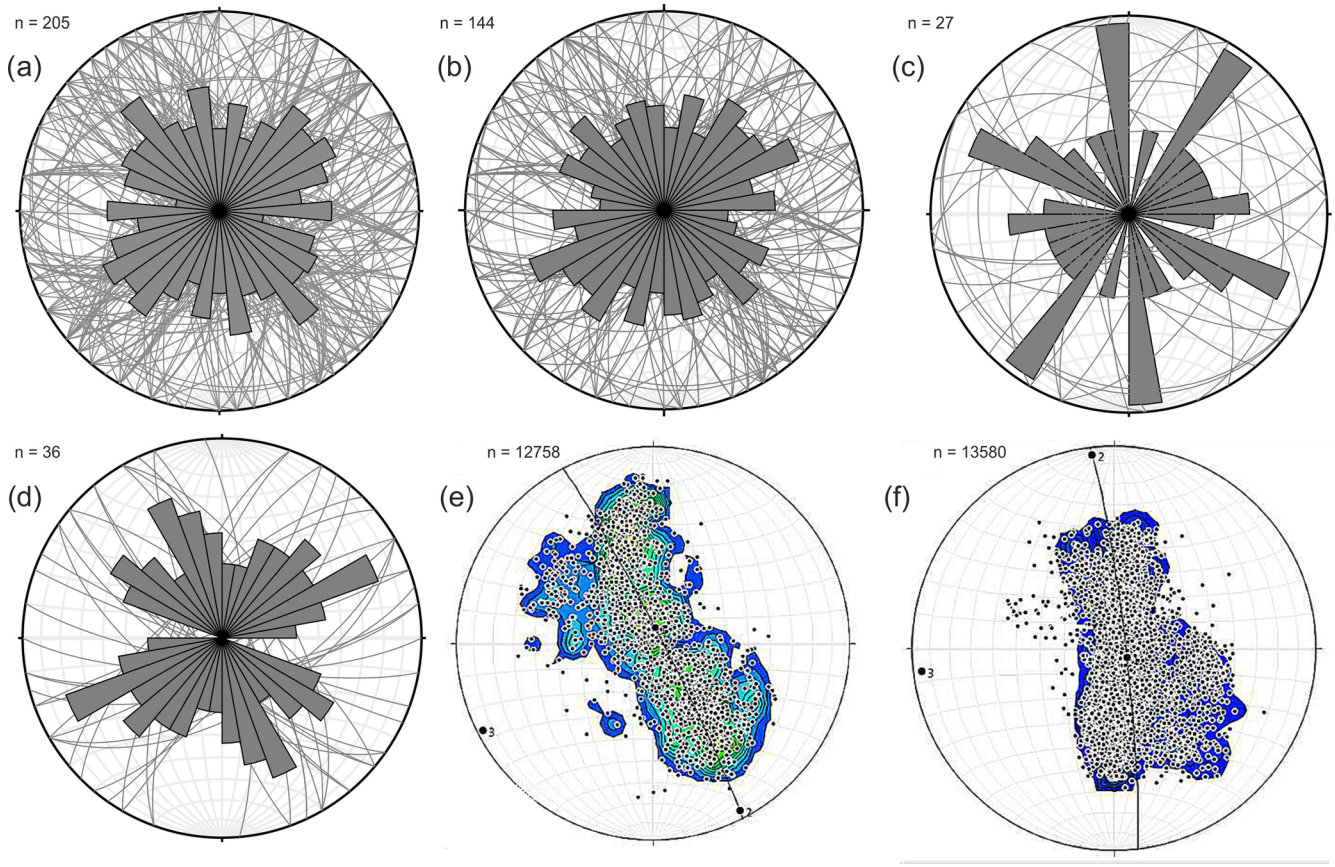

Figure 6. Stereoplot and rose diagrams (directions) of the fractures measured at the Como Roman baths: **(a)** all fractures, **(b)** fractures in stone and mortar, **(c)** chipped corners, **(d)** widening downward fractures, **(e)** facets' orientation extracted from the mesh of a single row of stones belonging to the first building phase, and **(f)** the same data for a row belonging to the second building phase.

In Lake Iseo, sediments were retrieved from the Sale Marasino sub-basin (Lauterbach et al., 2012) and from the main, deeper basin (Rapuc et al., 2022). In both cases, detrital event layers with metric thickness were identified and possibly related to seismic shaking. Rapuc et al. (2022) used geochemical proxies to distinguish extreme flood events from sediment accumulation driven by destabilization of slopes and delta. One event layer fits with the time frame of interest for our research: it is represented by a 1.4 m thick deposit, dated at 640–830 CE.

In Lake Garda, two major MTD beds were identified in the seismic stratigraphy, representing more than 50 % of the Holocene sedimentary record in the lake depocenter (Gasperini et al., 2020). Although the chronological constraints are highly speculative, one MTD layer is tentatively related to onshore evidence of surface faulting during the mid-third century CE at an archeological site at Egna (Adige Valley; Galadini and Galli, 1999).

In Lake Sils (Upper Engadine), an up to 6 m thick turbidite has been identified, with an estimated volume of 6.5×10^6 m^3; the top of the deposit is dated at 650–780 CE (Blass et al., 2005), while the peat layer underlying the event deposit is dated at 225–419 CE (Nigg et al., 2021). The megaturbidite extends over the entire lake and is interpreted as the result of a sudden collapse of the main delta entering the lake; it generated tsunami waves up to 5 m high, which inundated the lakeshore (Nigg et al., 2021).

Two sedimentary cores were retrieved from Lake Alzasca (Ticino region, Switzerland) and were analyzed to reconstruct the flood history. A complete Holocene succession was obtained, and the chronological constraints are supported by nine ^{14}C ages (Wirth, 2013). Two events listed by Kremer et al. (2020) overlap with the paleoseismic evidence dated at Como; their timing is derived from the nearest dated samples and the age–depth curve (Table 2).

A similar situation holds for Lake Cadagno (Ticino region, Switzerland), where two Holocene sediment successions were recovered from the deeper part of the basin. Nine ^{14}C dated samples provide chronological constraints to reconstruct the flood history (Wirth, 2013). Two events listed by Kremer et al. (2020) overlap with the paleoseismic evidence dated at Como.

Available data for Lake Lungern include a dense grid of high-resolution seismic lines and sedimentary cores (Mon-

Table 2. Summary of the positive evidence; see locations in Fig. 7.

Locality	Distance from Como (km)	Dates of the synchronous events (cal yr prob. 95 %)	Reference	Notes
Lake Como	15	500–600 CE	Fanetti et al. (2008)	date extrapolated
Lake Alzasca	63	633–816 CE	Wirth (2013)	offset from nearest dated sample: ∼ 210 years
Lake Alzasca	63	513–688 CE	Wirth (2013)	offset from nearest dated sample: ∼ 90 years
Lake Iseo	80	640–830 CE	Rapuc et al. (2022)	
Lake Sils	84	650–780 CE	Nigg et al. (2021)	
Lake Cadagno	87	579–963 CE	Wirth (2013)	offset from nearest dated sample: ∼ 0 years
Lake Cadagno	87	619–1006 CE	Wirth (2013)	offset from nearest dated sample: ∼ 40 years
Lake Engstlen	121	650–918 CE	Kremer et al. (2020)	offset from nearest dated sample: ∼ 230 years; uncertainties in composing the master core; dating not fully reliable (Katrina Kremer, personal communication, 2022)
Hinterburgsee	128	644 CE	Wirth (2013)	offset from nearest dated sample: ∼ 50 years (the evidence is unclear; Katrina Kremer, personal communication, 2022)
Lake Oeschinen	130	580–680 CE	Knapp et al. (2018)	
Lake Lungern	131	360–620 CE	Monecke et al. (2006)	offset from nearest dated sample in composite core: 5 years
Lake Lungern	131	380–800 CE	Monecke et al. (2006)	turbidite and mass flow on seismic reflection
Lake Lungern	131	520–730 CE	Monecke et al. (2006)	offset from nearest dated sample in composite core: 50 years

ecke et al., 2006). A total of 19 dated samples are used to derive an age–depth curve, which goes back up to about 2000 cal yr BP; three of the deformation horizons identified at Lake Lungern (LNG4, LNG5 and LNG6) have an age overlapping with the event dated at Como.

Knapp et al. (2018) apply sedimentology, radiocarbon dating and geophysics to investigate Lake Oeschinen (Swiss Alps). They found evidence of 11 rock-slope failure events, which in 4 cases have been related to (pre)historic earthquakes. Radiocarbon dating allowed us to reconstruct the local evolution in the last 2500 years; one of the events identified in Lake Oeschinen overlaps with the paleoseismic evidence at Como.

Table 2 includes also two entries from Lake Engstlen and Hinterburgsee; these data are less constrained than those of other lakes due to unclear dating or stratigraphic interpretation (Katrina Kremer, personal communication, 2022).

Figure 7b shows the age overlap among multiple sites, ordered according to their distance from the city of Como site. Blue dots represent positive evidence, whereas crosses indicate localities of negative evidence.

All the positive evidence overlaps with the upper and lower age limits for the paleoearthquake (Fig. 7b). If we consider a narrower time interval for the age of the paleoearthquake (i.e., within the max age of the lower limit and the min age of the upper limit), the overlapping events indicate a limited number of localities are correlated (e.g., Lake Como, Lake Alzasca, Lake Oeschinen and Lake Lungern) but still the distribution of these lakes overlaps with a more

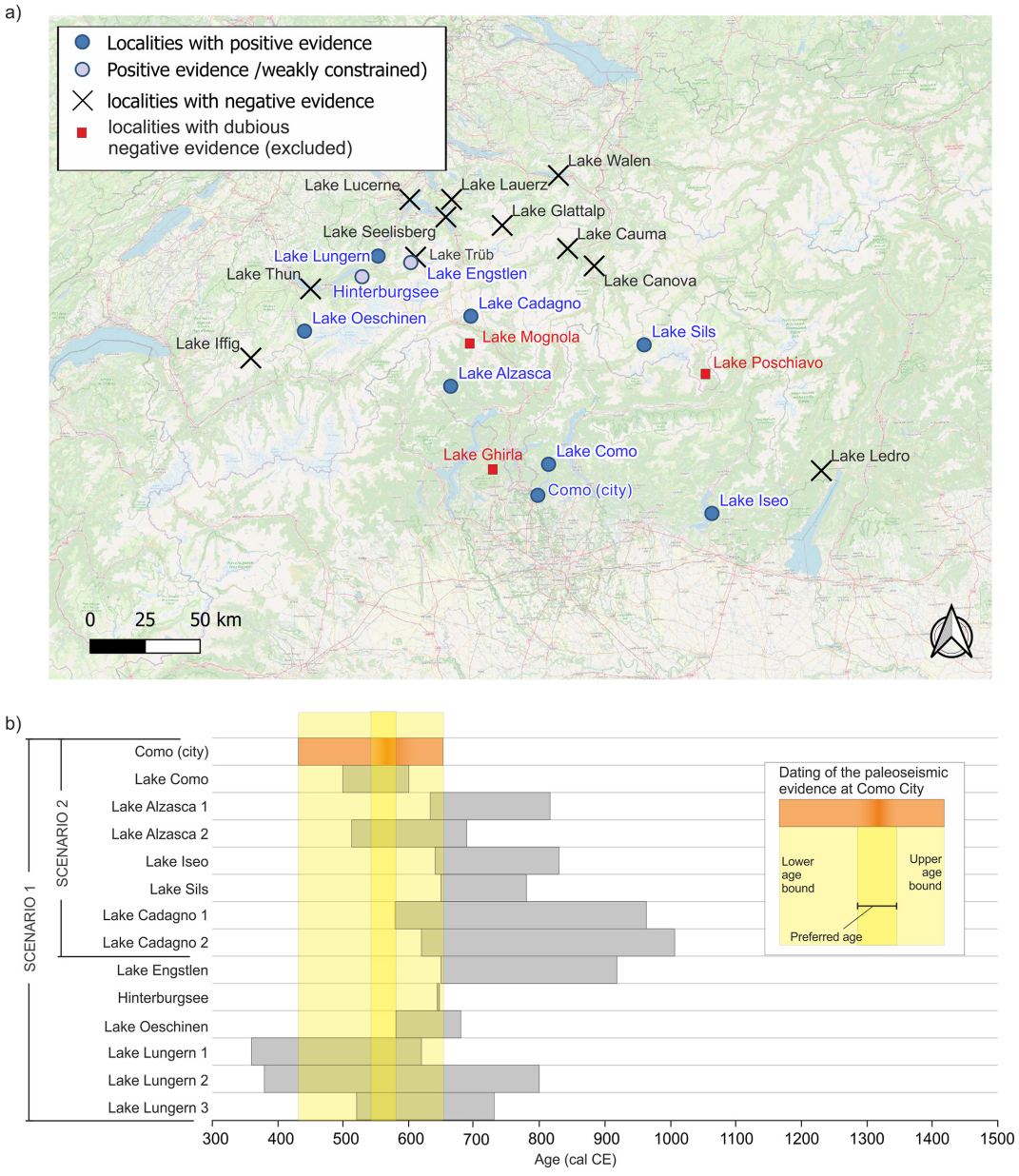

Figure 7. (a) Localities with positive and negative evidence for a synchronous effect caused by the sixth-century-CE earthquake (after the database available in Kremer et al., 2020); some of the localities have been excluded (red squares) due to incomplete stratigraphy or dubious evidence (see the text for details); basemap after © OpenStreetMap contributors 2023, distributed under the Open Data Commons Open Database License (ODbL) v1.0. **(b)** A comparison of the dated evidence at the city of Como with the age constraint for all the possible positive evidence of synchronous turbidites the Alpine lakes; age limits are given by the upper and lower boundary of the event age, given the age–depth curve calculated for any site and considering 2σ of confidence interval (data after Kremer et al., 2020, and available upon request to the authors).

inclusive scenario. As mentioned before, Lake Engstlen and Hinterburgsee suffer from higher uncertainty.

Some of the localities (red squares in Fig. 7) have been excluded due to their incomplete stratigraphy or to dubious evidence. These are Lake Mognola, Lake Ghirla and Lake Poschiavo.

At Lake Ghirla, located close to the City of Como, there are no events listed by Kremer et al. (2020) as possibly synchronous with the sixth-century-CE event. The stratigraphy of Lake Ghirla is well constrained by dating and records a continuous time window extending back to 13 ka (Wirth, 2013) with a dating located close to the time interval of interest. Nonetheless, a single episode of sedimentation with

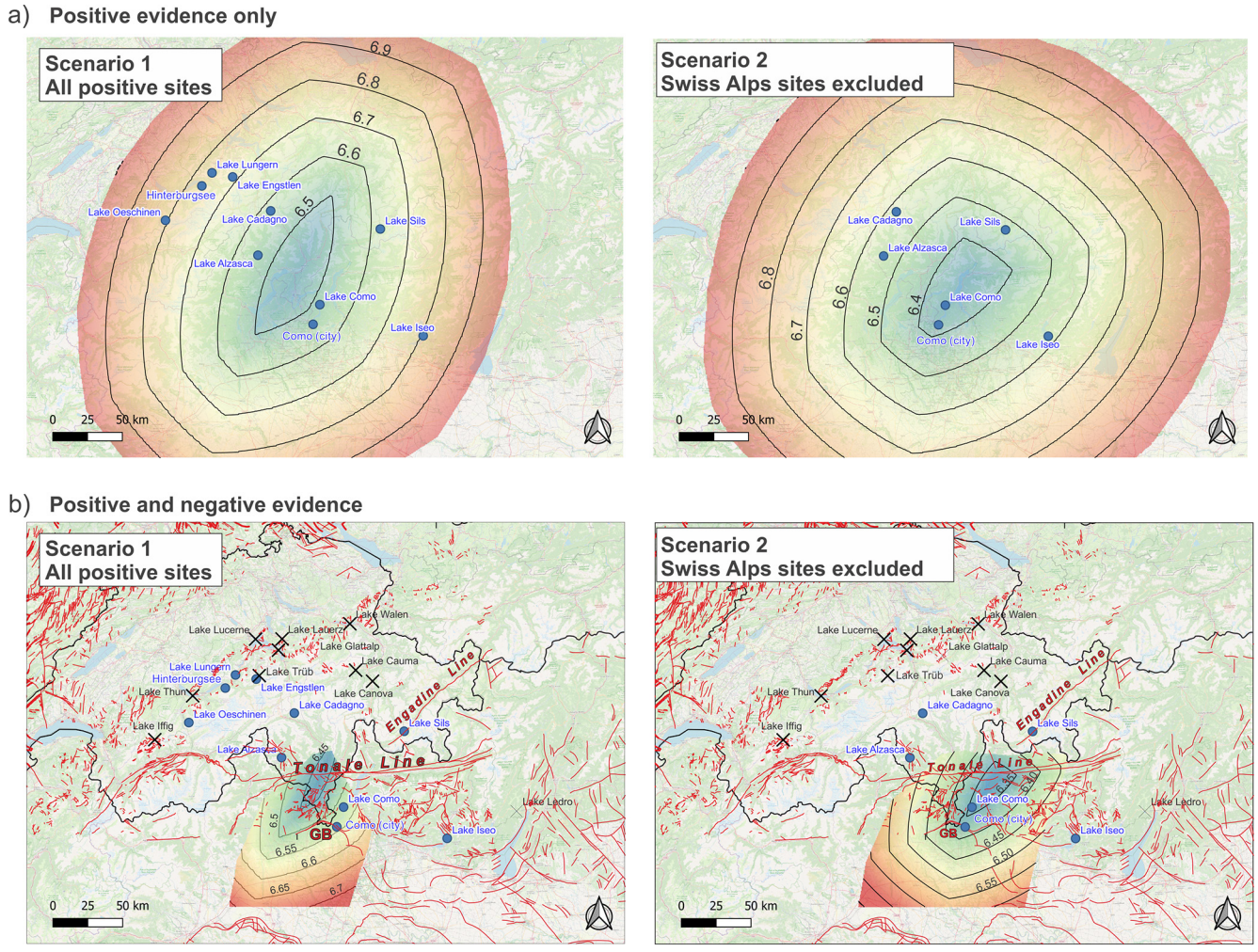

Figure 8. Results from the inverse grid search of the paleoearthquake, considering two possible scenarios of positive evidence (see text for details): **(a)** only positive evidence included; **(b)** positive and negative evidence included with a map of the potentially active faults of Switzerland (after Heténi et al., 2018) and capable faults for Italy (after Guerrieri et al., 2015; GB, Gonfolite backthrust). All basemaps after © OpenStreetMap contributors 2023. Distributed under the Open Data Commons Open Database License (ODbL) v1.0.

high detrital content is recorded close to the age of the paleoearthquake, possibly constituting positive evidence for such a small lake with a limited catchment. We thus found ambiguous evidence for this small lake and preferred to exclude it from any further analysis.

Lake Mognola is a small lake with a limited catchment as well. Its stratigraphic record, analyzed by Wirth (2013) for paleoclimate reconstructions, presents a peculiar stratigraphic record, not comparable with any other lake of the Southern Alps, which leads to the exclusion of this lake from further analyses. Possibly, these peculiarities emerge from the relatively high altitude of the site (2003 m a.s.l.) dominated by clastic and glacial geomorphologic processes. We thus excluded the site from our analysis as well.

Finally, Lake Poschiavo is characterized by very high sedimentation rates and the available stratigraphic record possibly does not reach the requested time window.

4.4 Potential source location

In the following analysis, we perform our calculations on two different datasets of positive evidence (Fig. 7b), resulting in two output scenarios (Fig. 8).

In Scenario 1 we used all the possible locations reporting positive evidence synchronous with the sixth-century-CE event; in Scenario 2 we excluded the locations in the Swiss Alps due to (i) their vicinity with other localities showing negative evidence instead, (ii) the reported uncertainties and limited overlap of the dated events from Lake Engstlen and Hinterburgsee, and (iii) the vicinity of other seismogenic sources (e.g., Fritsche et al., 2012; Strasser et al., 2013) that could be more probably invoked as sources for mass-wasting events in this area.

The inversion of the locations with positive and negative evidence of a paleoearthquake synchronous with the sixth-

century-CE event indicates a possible source located in the Southern Alps or close to the Periadriatic Line (Fig. 8). The minimum of the calculated earthquake magnitude is M_w 6.32 if we consider Scenario 2; in Scenario 1 the minimum magnitude is increased to M_w 6.43. Both the scenarios, when considered with the constraints of the negative-evidence locations, point to a similar area where the possible seismogenic source would have been located.

The area encompassing the minimum estimated M_w values (ca. M_w 6.4–6.5) is likely connected with the Tonale Line or other structures located close to the Italy–Switzerland border (Fig. 8b). Another possible candidate as a seismogenic source is the Gonfolite backthrust (GB in Fig. 8b), with a possible associated M_w of ca. 6.4: this fault has already been identified as potentially active (Michetti et al., 2012; Sileo et al., 2007).

Other possible sources should be located more to the south, associated with a higher magnitude range (M_w 6.6–6.7). This scenario seems less likely due to the absence of known active faults in the area. We underline that the lack of negative evidence to the south could be possibly ascribed to the lack of studies and stratigraphic records in the Po Plain sector.

5 Conclusions

The main conclusions of this study can be summarized as follows:

- We found deformations in a stratigraphic sequence and in an archeological site in the city of Como, dated at the sixth century CE. We interpret such deformations as evidence of earthquake ground shaking.
- We gathered information from the published literature for other sites in the western Southern Alps where paleoseismic evidence has been inferred in the same time interval.
- By applying an inverse-grid approach, we claim that an earthquake that is so far undocumented (minimum M_w 6.32) with an epicentral location at the border between Italy and Switzerland can explain the spatial pattern and distribution of paleoseismic evidence dated to the sixth century CE.
- Our study indicates the need to better evaluate the seismic risk in the western Southern Alps, a low-deformation region characterized by a high density of infrastructure and economic assets.
- Our results find some confirmation in the literature that deals with the seismotectonic potential of the Southern Alps. In an early study that made use of pattern recognition techniques in the study of the regional seismotectonics of the Alps, Cisternas et al. (1985) found a potentially hazardous area, directly in correspondence to the potential source location we identified (their area no. 15) and consistent with the results of Caputo et al. (1980) as well. Their potentially hazardous area lies at the intersection between the Tonale Line and a second-order transverse lineament, grossly corresponding to the Valchiavenna–Spluga valley.

While we were writing this paper, Bellwald et al. (2023) provided additional evidence: an event recorded at Lake Silvaplana (at only 2 km from Lake Sils) is synchronous with our evidence and points to the Engadine Line (Fig. 8) as a possible seismogenic source for the documented event. The Engadine Line, in fact, shows evidence of Holocene surface faulting and historical re-activations (Tibaldi and Pasquarè, 2008). Nonetheless, from the present analysis, the Engadine Line is apparently excluded as a possible candidate due to the constraints provided by the negative-evidence data points.

The papers described above prefer a location for the possible seismogenic source located in the Central Alps or close to the Insubric Line. As an alternative hypothesis, the source could be located, with a slightly higher magnitude, at the foothills of the Southern Alps, close to Lake Como and the city of Como. A seismogenic source, in this line, could be the Gonfolite backthrust (GB in Fig. 8; Michetti et al., 2012). Possible evidence, in this line, comes from the work after Fanetti and Vezzoli (2007). In this work a major fluvial diversion is dated back to the sixth century CE with the location of the outlet of a major stream running along the GB trace (Breggia River, 2 km NW of the city of Como; Fig. 2a), shifted to the south for the first and only time since the late glacial period. Notwithstanding the poor chronological constraints on such an event, the consistency of the timing is noteworthy. Historical sources report major flooding in the whole of northern Italy at that time, a period known in the scientific literature as the Late Antique Little Ice Age (Büntgen et al., 2016). Nonetheless, we cannot rule out that cascade-like events involving the occurrence of a strong earthquake with the consequent occurrence of numerous landslides, remobilization of large volumes of debris, available for water transportation, and intense and prolonged periods of rainfall could have triggered a chain of events inducing this major shift in the Breggia riverbed (e.g., Tang et al., 2012; Fan et al., 2018).

Data availability. The database of the paleoseismic evidence of Alpine lakes is included in Kremer et al. (2020).

Supplement. The supplement related to this article is available online at: https://doi.org/10.5194/nhess-23-3407-2023-supplement.

Author contributions. FL and EM collected the samples, described the stratigraphic sections and documented all the excavations at the Via Manzoni site; FL built the virtual 3D model of the Roman baths and analyzed the archeoseismological evidence with MFF; ST and SC analyzed and treated all the samples for dating; FL inverted the intensity data points for source location and magnitude calculations; AMM supervised the research and reviewed the manuscript; FL prepared the manuscript with contributions from all co-authors.

Competing interests. The contact author has declared that none of the authors has any competing interests.

Disclaimer. Publisher's note: Copernicus Publications remains neutral with regard to jurisdictional claims made in the text, published maps, institutional affiliations, or any other geographical representation in this paper. While Copernicus Publications makes every effort to include appropriate place names, the final responsibility lies with the authors.

Acknowledgements. We thank Giovanni Martinelli and Gerasimos Papadopoulos for fruitful comments and the editor for handling our manuscript. Katrina Kremer is acknowledged for having provided, upon request, the dataset in Kremer et al. (2017) and for fruitful discussion; the authors are indebted to SABAP (Soprintendenza Archeologia, Belle Arti e Paesaggio) of the Province of Como. Elisa Ticozzi, Federica Cozzula and Camilla Clerici are particularly thanked for having provided their time and effort and for contributing to this research: part of the results of this paper are the fruits of the results discussed in their theses.

Financial support. This research has been funded by the European Union – NextGenerationEU – Mission 4 "Education and Research" – Component 2 "From Research to Business" – Investment 3.1 "Fund for the realization of an integrated system of research and innovation infrastructures" – Project IR0000037 – GeoSciences IR.

Review statement. This paper was edited by Filippos Vallianatos and reviewed by Gerasimos Papadopoulos and Giovanni Martinelli.

References

Bakun, W. U. and Wentworth, C. M.: Estimating earthquake location and magnitude from seismic intensity data, Bull. Seismol. Soc. Am., 87, 1502–1521, 1997.

Beck, C.: Late Quaternary lacustrine paleo-seismic archives in north-western Alps: Examples of earthquake-origin assessment of sedimentary disturbances, Earth-Sci. Rev., 96, 327–344, https://doi.org/10.1016/j.earscirev.2009.07.005, 2009.

Bellwald, B., Nigg, V., Fabbri, S. C., Becker, L. W. M., Gilli, A., and Anselmetti, F. S. Holocene seismic activity in south-eastern Switzerland: Evidence from the sedimentary record of Lake Silvaplana, Sedimentology, https://doi.org/10.1111/sed.13131, in press, 2023.

Bernoulli, D., Bertotti, G., and Zingg, A.: Northward thrusting of the Gonfolite Lombarda ("South-Alpine Molasse") onto the Mesozoic sequence of the Lombardian Alps; implications for the deformation history of the Southern Alps, Eclog. Geolog. Helv., 82, 841–856, 1989.

Blass, A., Anselmetti, F. S., Grosjean, M., and Sturm, M.: The last 1300 years of environmental history recorded in the sediments of Lake Sils (Engadine, Switzerland), Eclog. Geol. Helv., 98, 319–332, https://doi.org/10.1007/s00015-005-1166-5, 2005.

Borgatti, L. and Soldati, M.: Landslides as a geomorphological proxy for climate change: a record from the Dolomites (northern Italy), Geomorphology, 120, 56–64, 2010.

Büntgen, U., Myglan, V. S., Ljungqvist, F. C., McCormick, M., Di Cosmo, N., Sigl, M., Jungclaus, J., Wagner, S., Krusic, P. J., Esper, J., Kaplan, J. O., de Vaan, M. A. C., Luterbacher, J., Wacker, L., Tegel, W., and Kirdyanov, A. V.: Cooling and societal change during the Late Antique Little Ice Age from 536 to around 660 ADA.D, Nat. Geosci., 9, 231–236, 2016.

Caputo, M., Keilis-Borok, V. I., Oficerova, E., Rauzman, E., Rotvain, I., and Soloviev, A.: Pattern recognition of earthquake-prone areas in Italy, Phys. Earth Planet. Int., 21, 305–320, 1980.

Casini, S.: Carta archeologica della Lombardia: La Provincia di Como, FC Panini Editore, ISBN 8876862110, 1994.

Castellarin, A., Vai, G. B., and Cantelli, L.: The Alpine evolution of the Southern Alps around the Giudicarie faults: A Late Cretaceous to Early Eocene transfer zone, Tectonophysics, 414, 203–223, https://doi.org/10.1016/j.tecto.2005.10.019, 2006.

Castelletti, L. and Motella De Carlo, S.: Il fuoco e la montagna. Archeologia del Paesaggio dal Neolitico all'Età Moderna in alta Val Cavargna, Castelletti, Lanfredo, Motella De Carlo, Sila, Como, 209 pp., 2012.

Cercatillo, S., Friedrich, M., Kromer, B., Paleček, D., and Talamo, S.: Exploring different methods of cellulose extraction for ^{14}C dating, New J. Chem., 45, 8936–8941, 2021.

Cisternas, A., Godefroy, P., Gvishiani, A., Gorshkov, A. I., Kossobokov, V., Lambert, M., Ranzman, E., Sallantin, J., Soldano, H., Soloviev, A., and Weber, C.: A dual approach to recognition of earthquake-prone areas in the western Alps, Ann. Geophys., 3, 249–270, 1985.

Comerci, V., Capelletti, S., Michetti, A. M., Rossi, S., Serva, L., and Vittori, E.: Land subsidence and Late Glacial environmental evolution of the Como urban area (Northern Italy), Quatern. Int., 173, 67–86, 2007.

Cremaschi, M.: Manuale di geoarcheologia, Laterza, ISBN 8842060259, 2000.

Fäh, D., Giardini, D., Kästli, P., Deichmann, N., Gisler, M., Schwarz-Zanetti, G., Alvarez-Rubio, S., Sellami, S., Edwards, B., and Allmann, B.: ECOS-09 earthquake catalogue of Switzerland release 2011 report and database, Public catalogue, 17.4.2011, Swiss Seismological Service ETH Zurich, RISK, http://ecos09.seismo.ethz.ch/index.html (last access: 30 October 2023), 2011.

Fan, X., Juang, C. H., Wasowski, J., Huang, R., Xu, Q., Scaringi, G., van Westen, C. J., and Havenith, H.-B.: What we have learned from the 2008 Wenchuan Earthquake and its aftermath: A decade of research and challenges, Eng. Geol., 241, 25–32, 2018.

Fanetti, D. and Vezzoli, L.: Sediment input and evolution of lacustrine deltas: The Breggia and Greggio rivers case study (Lake Como, Italy), Quatern. Int., 173, 113–124, 2007.

Fanetti, D., Anselmetti, F. S., Chapron, E., Sturm, M., and Vezzoli, L.: Megaturbidite deposits in the Holocene basin fill of Lake Como (Southern Alps, Italy), Palaeogeogr. Palaeocl., Palaeoecol., 259, 323–340, https://doi.org/10.1016/j.palaeo.2007.10.014, 2008.

Fantoni, R., Bersezio, R., and Forcella, F.: Alpine structure and deformation chronology at the Southern Alps-Po Plain border in Lombardy, Bollettino della Società geologica italiana, 123, 463–476, 2004.

Ferrario, M. F., Brunamonte, F., Caccia, A., Livio, F., Martinelli, E., Mazzola, E., Michetti, A. M., and Terrana, S.: Buried landscapes: geoarchaeology of the roman harbor of Como (N Italy), Alp. Mediterr. Quat., 111–120, http://amq.aiqua.it (last access: 30 October 2023), 2015.

Ferrater, M., Silva, P. G., Ortuño, M., Rodríguez-Pascua, M. Á., and Masana, E.: Archaeoseismological analysis of a Late Bronze Age site on the Alhama de Murcia fault, SE Spain, Geoarchaeology, 30, 151–164, 2015.

Fritsche, S., Fäh, D., and Schwarz-Zanetti, G.: Historical intensity VIII earthquakes along the Rhone valley (Valais, Switzerland): primary and secondary effects, Swiss J. Geosci., 105, 1–18, https://doi.org/10.1007/s00015-012-0095-3, 2012.

Galadini, F. and Galli, P.: Palaeoseismology related to the displaced Roman archaeological remains at Egna (Adige Valley, northern Italy), Tectonophysics, 308, 171–191, https://doi.org/10.1016/S0040-1951(99)00080-3, 1999.

Gallup, D., Frahm, J.-M., Mordohai, P., Yang, Q., and Pollefeys, M.: Real-time plane-sweeping stereo with multiple sweeping directions, in: 2007 IEEE Conference on Computer Vision and Pattern Recognition, 17–22 June 2007, 1–8, 2007.

Gasperini, L., Marzocchi, A., Mazza, S., Miele, R., Meli, M., Najjar, H., Michetti, A. M., and Polonia, A.: Morphotectonics and late Quaternary seismic stratigraphy of Lake Garda (Northern Italy), Geomorphology, 371, 107427, https://doi.org/10.1016/j.geomorph.2020.107427, 2020.

Giner-Robles, J. L., Rodríguez-Pascua, M. A., Pérez-López, R., Silva, P. G., Bardají, T., Grützner, C., and Reicherter, K.: Structural analysis of earthquake archaeological effects (EAE): Baelo Claudia examples (Cádiz, South Spain), in: 1st INQUA-IGCP International Workshop on Earthquake Archaeology and Paleoseismology, vol. 2, AEQUA – IGME, 2009.

Goesele, M., Snavely, N., Curless, B., Hoppe, H., and Seitz, S. M.: Multi-view stereo for community photo collections, in: 2007 IEEE 11th International Conference on Computer Vision, 1–8, https://doi.org/10.1109/ICCV.2007.4408933, 2007.

Guerrieri, L., Blumetti, A. M., Comerci, V., Manna, P. D., Michetti, A. M., Vittori, E., and Serva, L.: Surface Faulting Hazard in Italy: Towards a First Assessment Based on the ITHACA Database, in: Engineering Geology for Society and Territory – Volume 5, Springer, Cham, 1021–1025, https://doi.org/10.1007/978-3-319-09048-1_195, 2015.

Guidoboni, E., Comastri, A., and Phillips, B.: Catalogue of Earthquakes and Tsunamis in the Mediterranean Area from the 11th to the 15th Century, Istituto nazionale di geofisica e vulcanologia Rome, Italy, https://emidius.mi.ingv.it/ASMI/study/GUICO005 (last access: 30 October 2023), 2005.

Handy, M. R., Schmid, S. M., Bousquet, R., Kissling, E., and Bernoulli, D.: Reconciling plate-tectonic reconstructions of Alpine Tethys with the geological–geophysical record of spreading and subduction in the Alps, Earth-Sci. Rev., 102, 121–158, 2010.

Hetényi, G., Epard, J.-L., Colavitti, L., Hirzel, A. H., Kiss, D., Petri, B., Scarponi, M., Schmalholz, S. M., and Subedi, S.: Spatial relation of surface faults and crustal seismicity: a first comparison in the region of Switzerland, Acta Geod. Geophys., 53, 439–461, https://doi.org/10.1007/s40328-018-0229-9, 2018.

ISIDe Working Group: Italian seismological instrumental and parametric database (ISIDe), https://doi.org/10.13127/ISIDE, 2007.

Jorio, S.: Le terme di Como romana: seconda metà I-fine III secolo dC; testi dei pannelli didattici, Edizioni Et, Milano, ISBN 9788886752541, 2011.

Knapp, S., Gilli, A., Anselmetti, F. S., Krautblatter, M., and Hajdas, I.: Multistage rock-slope failures revealed in lake sediments in a seismically active Alpine region (Lake Oeschinen, Switzerland), J. Geophys. Res.-Earth, 123, 658–677, 2018.

Kremer, K., Wirth, S. B., Reusch, A., Fäh, D., Bellwald, B., Anselmetti, F. S., Girardclos, S., and Strasser, M.: Lake-sediment based paleoseismology: Limitations and perspectives from the Swiss Alps, Quaternary Sci. Rev., 168, 1–18, https://doi.org/10.1016/j.quascirev.2017.04.026, 2017.

Kremer, K., Gassner-Stamm, G., Grolimund, R., Wirth, S. B., Strasser, M., and Fäh, D.: A database of potential paleoseismic evidence in Switzerland, J. Seismol., 24, 247–262, https://doi.org/10.1007/s10950-020-09908-5, 2020.

Lauterbach, S., Chapron, E., Brauer, A., Hüls, M., Gilli, A., Arnaud, F., Piccin, A., Nomade, J., Desmet, M., von Grafenstein, U., and DecLakes participants: A sedimentary record of Holocene surface runoff events and earthquake activity from Lake Iseo (Southern Alps, Italy), Holocene, 22, 749–760, 2012.

Livio, F., Berlusconi, A., Chunga, K., Michetti, A. M., and Sileo, G.: New stratigraphic and structural evidence for Late Pleistocene surface faulting along the Monte Olimpino Backthrust (Lombardia, N Italy), Rend. Online Soc. Geol. It., 14, 17–25, https://doi.org/10.3301/ROL.2011.03, 2011.

Luraschi, G.: Storia di Como antica: saggi di archeologia, diritto e storia, New Press, ISBN 9788895383835, 1997.

Martinelli, E., Michetti, A. M., Colombaroli, D., Mazzola, E., Motella De Carlo, S., Livio, F., Gilli, A., Ferrario, M. F., Höbig, N., Brunamonte, F., Castelletti, L., and Tinner, W.: Climatic and anthropogenic forcing of prehistorical vegetation succession and fire dynamics in the Lago di Como area (N-Italy, Insubria), Quaternary Sci. Rev., 161, 45–67, https://doi.org/10.1016/j.quascirev.2017.01.023, 2017.

Martinelli, E., Michetti, A. M., Castelletti, L., Colombaroli, D., Ferrario, M. F., Livio, F. A., Motella De Carlo, S., and Tinner, W.: Il paesaggio preromano proto-urbano nei dintorni di Como: contesto ambientale e trasformazioni antropiche, Scenari di ricostruzione delle interazioni uomo-ambiente in Lombardia (N-Italia) dal Paleolitico medio all'età del Ferro, Firenze, 9–36, https://doi.org/10.1016/j.quascirev.2017.01.023, 2022.

Michetti, A., Giardina, F., Livio, F., Mueller, K., Serva, L., Sileo, G., Vittori, E., Devoti, R., Riguzzi, F., and Carcano, C.: Active compressional tectonics, Quaternary capable faults, and the seismic landscape of the Po Plain (N Italy), Ann. Geophys., 55, 969–1001, https://doi.org/10.4401/ag-5462, 2012.

Michetti, A. M., Livio, F. A., Pasquarè, F., Aligi, Vezzoli, L., Bini, A., Bernoulli, D., and Sciunnach, D.: Carta Geologica d'Italia, Foglio 075, Como, https://www.isprambiente.gov.it/Media/carg/75_COMO/Foglio.html (last access: 30 October 2023), 2014.

Monecke, K., Anselmetti, F. S., Becker, A., Schnellmann, M., Sturm, M., and Giardini, D.: Earthquake-induced deformation structures in lake deposits: A Late Pleistocene to Holocene paleoseismic record for Central Switzerland, Eclog. Geolog. Helv., 99, 343–362, 2006.

Nappo, N., Ferrario, M. F., Livio, F., and Michetti, A. M.: Regression analysis of subsidence in the Como Basin (Northern Italy): new insights on natural and anthropic drivers from InSAR data, Remote Sens., 12, 2931, https://doi.org/10.3390/rs12182931, 2020.

Nappo, N., Peduto, D., Polcari, M., Livio, F., Ferrario, M. F., Comerci, V., Stramondo, S., and Michetti, A. M.: Subsidence in Como historic centre (northern Italy): Assessment of building vulnerability combining hydrogeological and stratigraphic features, Cosmo-SkyMed InSAR and damage data, Int. J. Disast. Risk Reduct., 56, 102115, https://doi.org/10.1016/j.ijdrr.2021.102115, 2021.

Nigg, V., Wohlwend, S., Hilbe, M., Bellwald, B., Fabbri, S. C., de Souza, G. F., Donau F., Grischott, R., Strasser, M., and Anselmetti, F. S.: A tsunamigenic delta collapse and its associated tsunami deposits in and around Lake Sils, Switzerland, Nat. Hazards, 107, 1069–1103, 2021.

Oswald, P., Strasser, M., Hammerl, C., and Moernaut, J.: Seismic control of large prehistoric rockslides in the Eastern Alps, Nat. Commun., 12, 1059, https://doi.org/10.1038/s41467-021-21327-9, 2021.

Owen, G. and Moretti, M.: Identifying triggers for liquefaction-induced soft-sediment deformation in sands, Sediment. Geol., 235, 141–147, 2011.

Ramsey, C. B.: Bayesian analysis of radiocarbon dates, Radiocarbon, 51, 337–360, 2009.

Rapuc, W., Arnaud, F., Sabatier, P., Anselmetti, F. S., Piccin, A., Peruzza, L., Bastien, A., Augustin, L., Régnier, E., Gaillardet, J., and Von Grafenstein, U.: Instant sedimentation in a deep Alpine lake (Iseo, Italy) controlled by climate, human and geodynamic forcing, Sedimentology, 69, 1816–1840, https://doi.org/10.1111/sed.12972, 2022.

Reimer, P. J., Austin, W. E. N., Bard, E., Bayliss, A., Blackwell, P. G., Ramsey, C. B., Butzin, M., Cheng, H., Edwards, R. L., Friedrich, M., Grootes, P. M., Guilderson, T. P., Hajdas, I., Heaton, T. J., Hogg, A. G., Hughen, K. A., Kromer, B., Manning, S. W., Muscheler, R., Palmer, J. G., Pearson, C., Plicht, J. van der, Reimer, R. W., Richards, D. A., Scott, E. M., Southon, J. R., Turney, C. S. M., Wacker, L., Adolphi, F., Büntgen, U., Capano, M., Fahrni, S. M., Fogtmann-Schulz, A., Friedrich, R., Köhler, P., Kudsk, S., Miyake, F., Olsen, J., Reinig, F., Sakamoto, M., Sookdeo, A., and Talamo, S.: The IntCal20 Northern Hemisphere RADiocarbon Age Calibration Curve (0–55 cal kBP), Radiocarbon, 62, 725–757, https://doi.org/10.1017/RDC.2020.41, 2020.

Rodríguez-Pascua, M. A., Pérez-López, R., Giner-Robles, J. L., Silva, P. G., Garduño-Monroy, V. H., and Reicherter, K.: A comprehensive classification of Earthquake Archaeological Effects (EAE) in archaeoseismology: Application to ancient remains of Roman and Mesoamerican cultures, Quatern. Int., 242, 20–30, 2011.

Rotondi, R. and Garavaglia, E.: Statistical analysis of the completeness of a seismic catalogue, Nat. Hazards, 25, 245–258, 2002.

Rovida, A., Locati, M., Camassi, R., Lolli, B., and Gasperini, P.: Catalogo Parametrico dei Terremoti Italiani, versione CPTI15, release 1.5, 33, INGV, https://doi.org/10.6092/INGV.IT-CPTI15, 2016.

Scaramuzzo, E., Livio, F. A., Granado, P., Di Capua, A., and Bitonte, R.: Anatomy and kinematic evolution of an ancient passive margin involved into an orogenic wedge (Western Southern Alps, Varese area, Italy and Switzerland), Swiss J. Geosci., 115, 4, https://doi.org/10.1186/s00015-021-00404-7, 2022.

Schmid, S. M. and Kissling, E.: The arc of the western Alps in the light of geophysical data on deep crustal structure, Tectonics, 19, 62–85, https://doi.org/10.1029/1999TC900057, 2000.

Sileo, G., Giardina, F., Livio, F., Michetti, A. M., Mueller, K., and Vittori, E.: Remarks on the Quaternary tectonics of the Insubria Region (Lombardia, NW Italy, and Ticino, SE Switzerland), Bollettino-Societa Geologica Italiana, 126, 411–425, 2007.

Strasser, M., Anselmetti, F. S., Fäh, D., Giardini, D., and Schnellmann, M.: Magnitudes and source areas of large prehistoric northern Alpine earthquakes revealed by slope failures in lakes, Geology, 34, 1005–1008, https://doi.org/10.1130/G22784A.1, 2006.

Strasser, M., Monecke, K., Schnellmann, M., and Anselmetti, F. S.: Lake sediments as natural seismographs: A compiled record of Late Quaternary earthquakes in Central Switzerland and its implication for Alpine deformation, Sedimentology, 60, 319–341, https://doi.org/10.1111/sed.12003, 2013.

Stucchi, M., Albini, P., Mirto, M., and Rebez, A.: Assessing the completeness of Italian historical earthquake data, Ann. Geophys., 47, 659–673, https://doi.org/10.4401/ag-3330, 2004.

Tang, C., van Asch, T. W., Chang, M., Chen, G. Q., Zhao, X. H., and Huang, X. C.: Catastrophic debris flows on 13 August 2010 in the Qingping area, southwestern China: the combined effects of a strong earthquake and subsequent rainstorms, Geomorphology, 139, 559–576, 2012.

Tibaldi, A. and Pasquarè, F. A.: Quaternary deformations along the 'Engadine–Gruf tectonic system', Swiss–Italian Alps, J. Quaternary Sci., 23, 475–487, 2008.

Trauth, M. H., Bookhagen, B., Marwan, N., and Strecker, M. R.: Multiple landslide clusters record Quaternary climate changes in the northwestern Argentine Andes, Palaeogeogr. Palaeocl. Palaeoecol., 194, 109–121, https://doi.org/10.1016/S0031-0182(03)00273-6, 2003.

Uboldi, M.: Carta archeologica della Lombardia, Como, La città murata e la convalle, Franco Cosimo Panini, Modena, ISBN 9788876862328, 1993.

Westoby, M. J., Brasington, J., Glasser, N. F., Hambrey, M. J., and Reynolds, J. M.: 'Structure-from-Motion' photogrammetry: A low-cost, effective tool for geoscience applications, Geomorphology, 179, 300–314, 2012.

Wirth, S. B.: The Holocene flood history of the central Alps reconstructed from lacustrine sediments: frequency, intensity and controlling climate factors, PhD Thesis, ETH Zurich, Zurich, https://doi.org/10.3929/ethz-a-009775044, 2013.

Zanchetta, S., Malusà, M. G., and Zanchi, A. M.: Precollisional development and Cenozoic evolution of the Southalpine retrobelt (European Alps), Lithosphere, 7, 662–681, https://doi.org/10.1130/L466.1, 2015.